THE ANATOLIAN JOURNAL OF CARDIOLOGY

Official journal of the TURKISH SOCIETY OF CARDIOLOGY

A Supervised Learning Approach Electrocardiographic Model for Differentiating Outflow Tract Premature Ventricular Complex Origins: Comparative Analysis of Seven Established Algorithms

ABSTRACT

Background: Premature ventricular complexes (PVCs) arising from the right and left ventricular outflow tracts (RVOT and LVOT) require accurate localization for successful ablation. Existing electrocardiographic (ECG) algorithms are limited by anatomical variability. This study aimed to develop a supervised learning approach model based on logistic regression using validated ECG parameters and to compare its diagnostic performance with 7 established algorithms.

Methods: A retrospective cohort of 116 patients with idiopathic outflow tract PVCs who underwent successful ablation between 2015 and 2020 was analyzed. Four ECG parameters were selected through backward stepwise logistic regression. The performance of the model and 7 published algorithms was assessed using receiver-operating characteristic (ROC) curve analysis, Youden index, and accuracy metrics. Subgroup analysis was performed in patients with V3 precordial transition.

Results: The supervised learning model achieved the highest diagnostic accuracy with an area under the ROC curve of 0.942 in the overall cohort and 0.878 in the V3 transition subgroup, significantly outperforming all comparator algorithms ($P < .001$). The model demonstrated a Youden index of 0.66, sensitivity of 82.7%, and specificity of 84.4%.

Conclusion: The supervised learning approach model outperformed existing rule-based ECG algorithms in differentiating RVOT from LVOT PVCs. By integrating validated ECG features into a statistically optimized and interpretable framework, it provides a reliable noninvasive tool to support ablation planning. Larger multicenter validation studies are warranted.

Keywords: Arrhythmias, artificial intelligence, cardiac, catheter ablation, electrocardiography, logistic models, machine learning, premature ventricular contractions

ORIGINAL INVESTIGATION

INTRODUCTION

Premature ventricular complexes (PVCs) are common arrhythmic events associated with an increased risk of reduced left ventricular (LV) ejection fraction, heart failure, and all-cause mortality.[1] In patients with structurally normal hearts, idiopathic PVCs most frequently originate from the right or left ventricular outflow tracts (RVOT/LVOT). When pharmacologic therapy is ineffective or poorly tolerated, catheter ablation emerges as an effective and well-established treatment option. Outflow tract ventricular arrhythmias can be safely and efficiently targeted using radiofrequency (RF) catheter ablation, which achieves high long-term success rates.[2] Accurate focus localization is essential, yet RVOT–LVOT differentiation remains difficult due to their close anatomical proximity—especially near the aortomitral continuity—resulting in limited accuracy of current electrocardiographic (ECG)-based algorithms. Although several ECG algorithms have been developed to aid in PVC localization, many are based on fixed cutoff values derived from small cohorts, and their applicability across diverse populations remains inconsistent.[3-9] Existing ECG algorithms may be insufficient in complex

Ali Sezgin[1]
Cem Çöteli[2]
Ahmet Kıvrak[2]
Ugur Canpolat[2]
Necla Özer[2]
Hikmet Yorgun[2]
Kudret Aytemir[2]
Ahmet Hakan Ateş[2]

[1]*Department of Cardiology, Etlik City Hospital, Ankara, Türkiye*
[2]*Department of Cardiology, Faculty of Medicine, Hacettepe University, Ankara, Türkiye*

Corresponding author:
Ali Sezgin
✉ ali_sezgin_666@hotmail.com

Received: October 3, 2025
Accepted: February 24, 2026
Available Online Date: April 2, 2026

Cite this article as: Sezgin A, Çöteli C, Kıvrak A, et al. A supervised learning approach electrocardiographic model for differentiating outflow tract premature ventricular complex origins: comparative analysis of seven established algorithms. *Anatol J Cardiol.* 2026;XX(X):X-X.

DOI: 10.14744/AnatolJCardiol.2026.5770

cases, prompting us to re-evaluate key features and develop an integrated logistic regression-based supervised learning approach model. Supervised learning approach is a method that learns patterns from labeled data, much like a clinician recognizing risk by reviewing past cases with known outcomes. Using this approach, validated ECG markers were combined into a simple and interpretable tool for distinguishing RVOT from LVOT PVCs. A supervised learning approach model was developed based on logistic regression to distinguish RVOT from LVOT PVCs, and it was compared with 7 prior algorithms, aiming to provide a more accurate and practical tool for PVC localization and ablation planning.

METHODS

Dataset

The study retrospectively reviewed 370 patients who underwent PVC ablation between January 2015 and June 2020. Exclusion criteria included the absence of electrophysiologic study data, structural heart disease, baseline bundle branch block, non-outflow tract PVCs, unsuccessful ablation, and ECGs with evidence of improper V1–V2 lead placement. Appropriate precordial lead positioning was confirmed using indirect ECG criteria, including physiologic P-wave morphology, normal precordial R-wave progression, and the absence of patterns suggestive of high chest placement (e.g., unusually dominant R waves or atypical rSr′ in V1–V2). A total of 22 ECGs were excluded due to suspected improper V1–V2 lead placement, based on the predefined ECG criteria. After applying these criteria, 116 patients with LBBB morphology and an inferior axis were included in the final dataset for model development (Figure 1). To ensure methodological consistency, the study included only PVCs with an LBBB morphology and inferior axis, which is the phenotype used in most previously published RVOT–LVOT differentiation algorithms. This approach allowed direct comparison with existing tools and prevented heterogeneity related to other PVC morphologies.

This study was conducted in accordance with institutional and national ethical standards. Approval for the retrospective analysis was obtained from the Institutional Ethics Committee on January 19, 2021 (Approval Number: GO 21/79, 2021/02-43). As the study involved a retrospective review of clinical records acquired during routine care, the requirement for additional study-specific patient consent was waived. All patients had previously provided informed consent for their ablation procedures, and no directly identifiable personal information was used during data analysis.

Electrophysiologic Study and Ablation Procedure

All antiarrhythmic pharmacotherapies were terminated at least 5 half-lives before the ablation to guarantee drug elimination. The ablation procedure was performed only under local anesthesia. In all patients, a coronary sinus catheter was placed. Electroanatomical mapping was performed using a 3.5-mm open-irrigated ThermoCool catheter (Biosense Webster, Diamond Bar, CA, USA) in conjunction with the CARTO 3 (Biosense Webster, Irvine, CA, USA) or EnSite Precision (Abbott Medical, St. Paul, MN, USA) 3D mapping systems. The earliest activation site was determined from the surface QRS, and precocity was manually confirmed using the 3D mapping system and the Prucka/CardioLab EP recording system (GE Healthcare, Milwaukee, WI, USA). Radiofrequency energy was delivered to the earliest activation site, and the region where PVC originated was identified by the termination of PVC with RF energy. Additionally, heparin was given intravenously to keep the active clotting time over 300 seconds during mapping in the LVOT. Acute ablation success was defined as the complete elimination of the targeted clinical PVC during the electrophysiology procedure and persisting for at least 30 minutes after the final RF energy application, both at baseline and following isoproterenol infusion. Additionally, the absence of PVCs was confirmed through continuous full-disclosure telemetry monitoring for 24 hours post ablation during inpatient observation. Long-term procedural success was defined as a ≥80% reduction in the burden of the targeted PVC morphology on 24-hour Holter monitoring at 3-6 months of follow-up, in the absence of antiarrhythmic drug escalation or repeat ablation. All patients were routinely followed with outpatient clinic visits, including ECG and HF evaluation at 1, 3, and 6 months. Any recurrence of clinical PVCs was also assessed symptomatically and via rhythm monitoring, as appropriate.

Electrocardiographic Analysis

All ECG measurements and algorithm calculations were performed manually by a single experienced observer who was blinded to the ablation results, following the exact definitions and cutoff criteria provided in the original publications. A standard sweep speed of 25 mm/s and a voltage calibration of 10 mm/mV 12-lead ECGs were obtained for all patients during sinus rhythm and episodes of PVCs (Figure 2). These recordings were conducted using the conventional

HIGHLIGHTS

- A novel logistic regression–based electrocardiographic (ECG) model was developed to differentiate left vs. right ventricular outflow tract origins of premature ventricular complexes (PVCs).
- The model demonstrated superior diagnostic accuracy (area under the curve (AUC) 0.942 in all patients; AUC 0.878 in V3 transitional cases) compared with 7 established algorithms.
- Unlike conventional criteria, all parameters of the new model are derived from PVC morphology, making it independent of sinus QRS morphology and cardiac rotation.
- Conventional algorithms were limited in transitional cases, whereas the proposed model maintained consistent performance.
- This study suggests that the supervised learning approach to ECG analysis can enhance the localization of outflow tract PVCs and guide ablation strategies.

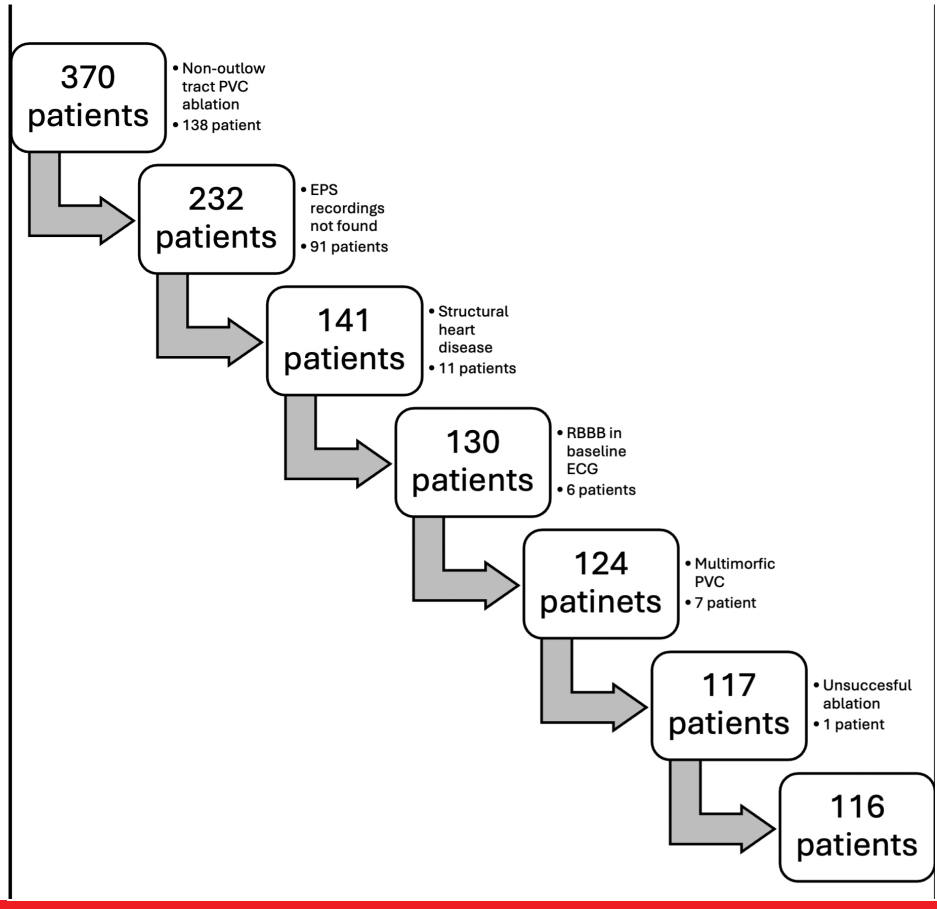

Figure 1. Flow chart of study population. A total of 370 patients undergoing premature ventricular complex (PVC) ablation between January 2015 and June 2020 were screened. After exclusions, 116 patients with idiopathic outflow tract PVCs were included in the analysis.

arrangement of the limb and chest leads. Special attention was given to the accurate placement of the electrodes for leads V1 and V2 in the fourth intercostal space to avoid erroneous positioning, which could significantly alter the QRS morphology associated with outflow tract ventricular arrhythmias. LBBB morphology was defined in accordance with American Heart Association / American College of Cardiology Foundation / Heart Rhythm Society recommendations, including a predominantly negative QRS complex in lead V1 (S wave amplitude exceeding the R wave) and a broad, notched, or slurred R wave in lateral leads.[10] An inferior axis was defined by a positive net QRS vector in leads II, III, and aVF, consistent with standard ECG criteria. Measurements were conducted using an electronic caliper within the recording system. To differentiate between right and left ventricular origins of PVCs, several ECG algorithms have been published. In the study, an analysis was conducted using 7 algorithms that are the most frequently used in previous studies, aiming to evaluate their effectiveness and accuracy in localizing the origin of PVCs. A total of 7 previously published algorithms were selected based on their availability at the time of study design (2020–2022), their validation in LBBB–inferior axis outflow-tract PVC cohorts, and their reliance on standard 12-lead ECG measurements. Features extracted from those 7 algorithms were used for model input. The selected parameters included:

1. V1 R wave amplitude: Vertical distance between the apex of the R wave and the isoelectric line.
2. V1 S wave amplitude: Vertical distance between the nadir of the S wave and the isoelectric line.
3. V1 QRS amplitude: Sum of the R and S wave amplitudes.
4. V2 R wave amplitude: Vertical distance between the peak of the R wave and the isoelectric line.
5. V2 S wave amplitude: Vertical distance between the nadir of the S wave and the isoelectric line.
6. V2 QRS amplitude: Sum of the R and S wave amplitudes.
7. V3 R wave amplitude: Vertical distance between the peak of the R wave and the isoelectric line.
8. Sinus V2 R amplitude: Vertical distance in the preceding sinus beat between the peak of the R wave and the isoelectric line in V2 derivation.
9. Sinus V2 QRS amplitude: Vertical distance in the preceding sinus beat between the peak of the R wave and the nadir of the S wave in V2 derivation.
10. PVC QRS duration: Horizontal distance from the earliest activation in any lead to the last one in any lead.
11. Sinus QRS amplitude: Vertical distance from the earliest activation of the preceding sinus beat in any lead to the last one in any lead.
12. V1 R wave duration: Horizontal distance from the first upward directed activation to the point where this wave intersects the isoelectric line.

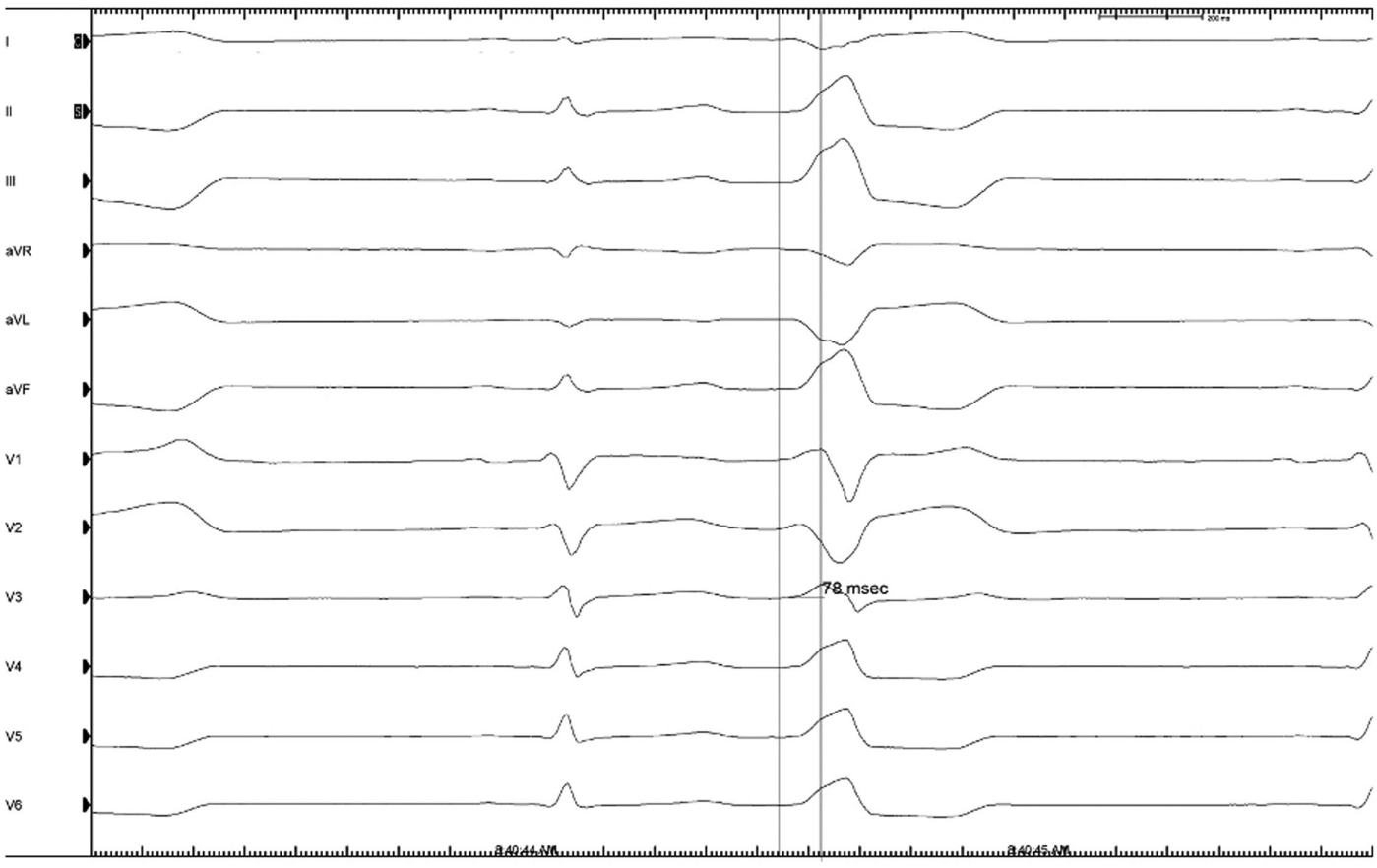

Figure 2. Example of right ventricular outflow tract free wall originated premature ventricular complex and V3 R wave deflection interval measurement. Representative 12-lead electrocardiograph showing measurement of the R-wave deflection interval in lead V3.

13. V2 R wave duration: Horizontal distance from the first upward directed activation to the point where this wave intersects the isoelectric line.
14. PVC Transition Zone (TZ) score: The number of chest leads in which the R wave amplitude of PVC is equal to or greater than the S wave amplitude of PVC.
15. Sinus TZ score: The number of chest leads in which the R wave amplitude of the sinus beat is equal to or greater than the S wave amplitude of the sinus beat.

Statistical Analysis

Statistical analyses were conducted using IBM SPSS Statistics for Windows, version 26.0 (IBM Corp., Armonk, NY, USA) with a 95% CI. For numerical variables, mean (M), standard deviation (SD), minimum, maximum, and median values are reported; for categorical variables, frequencies (n) and percentages (%) are presented. The chi-square test was used to evaluate relationships between categorical variables. Between-group comparisons were performed using independent i-tests or Mann–Whitney *U*-tests, based on the distribution of the data. Normality was assessed using both skewness/kurtosis values (with thresholds between ±3) and formal tests including the Shapiro–Wilk and Kolmogorov–Smirnov tests. Parametric or non-parametric methods were applied accordingly.

To identify key predictors of PVC origin and develop a classification model, a supervised learning approach approach based on binary logistic regression was employed. The classification problem was defined by labeling the left LVOT origin as 1 and the RVOT origin as 0. All candidate predictor variables—derived from established ECG algorithms—were initially included in the model. Because LVOT and RVOT cases were relatively balanced in the dataset, no class-balancing techniques or resampling were applied, and the full dataset was used for model derivation without a train–test split or cross-validation.

To optimize model performance and reduce overfitting risk, a backward stepwise logistic regression analysis (Wald test-based) was used. Through 8t iterative steps, non-significant variables were systematically removed based on predefined statistical criteria ($P > .05$). The final model retained only those predictors with statistically significant contributions, and model fit at each step was evaluated using the likelihood-ratio chi-square test. The statistical significance of the final model ($P < .05$) confirmed its robustness and predictive validity.

The diagnostic performance of the newly derived machine learning model was assessed using receiver operating characteristic (ROC) curve analysis. In addition to the new model,

ROC analyses were performed for 7 previously published ECG-based algorithms. The area under the curve (AUC) was calculated for each method, and pairwise AUC comparisons were conducted using the DeLong test. To evaluate the overall discriminative power of each model, the Youden Index was calculated. These performance metrics were computed for both the entire patient cohort and the V3 precordial transition subgroup.

RESULTS

The study included 116 participants, with 59 (51%) males. The average age was 45.8 years (±14.6). Most participants (87.7%) had no history of ablation, while 12.3% had undergone the procedure before. Of the 116 patients in the study, 63 (54.3%) underwent ablation for LVOT-origin PVCs, while 53 (45.7%) had RVOT-origin PVCs (Table 1).

Among the 63 patients who underwent LVOT ablation, the most targeted site was the left coronary cusp (LCC) in 21 patients (33.3%), followed by the right-left coronary cusp (RCC-LCC) junction in 17 patients (27.0%), and the LV summit region in 13 patients (20.6%). In the RVOT ablation group (n = 53), the most frequently ablated site was the RVOT anteroseptal region in 15 patients (28.3%), followed by the RVOT posteroseptal region in 10 patients (18.9%). Additionally, the RVOT anterior and posterior regions were each targeted in 9 patients (17.0%). This distribution illustrates the predominant ablation sites within the LVOT and RVOT groups among the study cohort. In the population, 13 patients (20.6% of LVOT cases) were classified as having PVCs originating from the LV summit. However, none of these ablations were performed via an epicardial approach. Instead, successful ablation was achieved from adjacent endocardial locations such as the aortic cusps or the subvalvular LVOT, where earliest activation was recorded and effective RF energy delivery was possible. These areas likely represent endocardial breakout points of summit-originating PVCs.

Table 1. Baseline Characteristics

Sex	
Male (%)	59 (50.9)
Female (%)	57 (49.1)
Age (years)	
Mean	45.8 ± 14.6
BMI (kg/m²)	
Mean	25.7 ± 11.4
LVEF (%)	
Mean	62.1 ± 4.3
LV end diastolic diamater (cm)	
Mean	4.5 ± 0.5 cm
Creatinine (mg/dL)	
Mean	0.83 ± 0.12
Hemoglobin (g/dL)	
Mean	13.5 ± 0.84
VT	
Yes (%)	8 (6.9)
No (%)	108 (93.1)
Previous ablation history	
Yes (%)	14 (12.3)
No (%)	102 (87.7)

Values are presented as mean ± standard deviation (SD) or number (percentage).
BMI, body mass index; LV, left ventricle; LVEF, left ventricular ejection fraction; VT, ventricular tachycardia.

Quantitative features derived from algorithms that discriminate right or left origin for PVC were compared between RVOT and LVOT ablation groups (Table 2). The RVOT group demonstrated statistically higher values in PVC TZ score, PVC QRS duration, PVC S wave amplitude in V1, PVC QRS amplitude in V1, PVC S wave amplitude in V2, and PVC QRS amplitude in V2, indicating greater wave amplitude and QRS complex duration in this group. Conversely, the LVOT group exhibited significantly higher values in the PVC R wave deflection interval in V3, PVC R wave amplitude in V2, and PVC R wave amplitude in V3, reflecting distinct patterns of R wave morphology in this region (Table 3).

The diagnostic performance of feature-based classification models was assessed using standard evaluation metrics, including sensitivity, specificity, positive predictive value (PPV), and negative predictive value (NPV). These metrics were calculated both for the overall dataset and for a clinically relevant subgroup of patients with a precordial transition at lead V3. In the full cohort, the Combined TZ Index–based model achieved the highest sensitivity (90.5%) and NPV (85.4%), indicating a robust capacity for identifying true LVOT cases while minimizing false negatives. Alternatively, the model incorporating the R Wave Duration Index and R/S Amplitude Index yielded the highest specificity (98.1%) and PPV (94.7%), reflecting strong discriminatory power for RVOT origin and low false positive rates. When applied to the V3 transition subgroup, the Combined TZ Index again demonstrated superior sensitivity (95.2%) and NPV (82.4%), whereas the R Wave Duration Index and R/S Amplitude Index model achieved perfect specificity and PPV (100% each), effectively eliminating false positives within this subgroup (Table 4).

All ECG algorithms showed statistically significant effectiveness in predicting the exact ablation location, confirming their utility in clinical settings (Table 5).

Building upon the diagnostic insights derived from individual ECG algorithms, a supervised learning approach model was developed using logistic regression to integrate the most informative features. The final model incorporated 4 key predictors: PVC TZ score, PVC V2 R wave duration, PVC V3 R wave amplitude, and PVC V2 S wave amplitude—all of which demonstrated independent discriminatory power in differentiating LVOT from RVOT origins (Table 6).

The logistic regression function was defined as: $Y = 8.436 - 2.036 \times \text{PVC TZ score} - 0.06 \times \text{PVC V2 R wave duration} + 4.661 \times \text{PVC V3 R wave amplitude} - 1.958 \times \text{PVC V2 S wave amplitude}$, with a threshold of $Y > 0.5$ indicating an LVOT origin (Figure 3; Table 7).

Table 2. Analyzed Algorithms in the Study

R wave amplitude index in V1 combining with R wave deflection interval in V3
If the ratio of R wave amplitude in V1 to QRS amplitude in V1 is >0.3 and the duration from the beginning of the R wave to the peak of the R wave in lead V3 > 80 ms, the origin is RVOT with the accuracy of 91.7%.
V2 transition ratio
If sinus rhythm is seen before than PVC, it is RVOT originated with %100 ratio, if R/S transition in PVC before the sinus rhythm, the amplitude ratio of PVC R/R+S in V2 must be divided by the preceding sins beat amplitude ratio of R/R+S. Result under 0.6 shows RVOT origin with sensitivity 95%, specificity 100%.
V2S/V3R Index
Ratio of S wave amplitude of PVC in V2 derivation and R wave amplitude of PVC in V3 derivation. Using a cut-off value of ≤1.5, this ECG algorithm predicted LVOT origin with a sensitivity of 89% and a specificity of 94%.
Transition Zone Index
The number of chest lead which R wave amplitude is equal or greater than S wave is defined TZ score. To find the TZ index, the TZ score of the PVC is mathematically subtracted from the TZ score in sinus rhythm. A TZ index cutoff value of <0 predicted ASC origin with a sensitivity of 88% and specificity of 82%.
Combined TZ and V2S/V3R Index
This is a mathematical formula that calculates a constant value by using TZ index and V2S/V3R index ($Y = -1.15 \times (TZ) - 0.494 \times (V2S/V3R)$). The model was prospectively tested in 207 patients, achieving a sensitivity of 90% and a specificity of 87% for LVOT origin.
SS and R wave difference in V1 and V2
This algorithm is a mathematical formula that subtracts sum of R wave amplitudes of V1 and V2 from sum of S wave amplitudes in V1 and V2. The ROC curve analysis determined a cutoff value of 1.625 mV for the V1-2 SRd to predict RVOT origin, with a sensitivity of 95.1%, specificity of 85.5%, positive predictive value of 86.5%, and negative predictive value of 94.5%.
R wave duration index and R/S wave amplitude index
The ratio of the R wave durations to the QRS durations in leads V1 and V2 is taken, and whichever is greater is accepted as the R wave duration index. R and S wave ratios in leads V1 and V2 are taken, and the greater R/S ratio is accepted as amplitude index. This algorithm was later tested prospectively in a cohort of 88 patients, demonstrating an overall sensitivity of 88% and specificity of 95%. The PPV was 88%, while the NPV was 96%.

ASC, aortic sinus cusp; LVOT, left ventricular outflow tract; NPV, negative predictive value; PPV, positive predictive value; PVC, premature ventricular complex; ROC, receiver operating characteristic; RVOT, right ventricular outflow tract; TZ, transition zone.

Table 3. Comparison of the Quantitative Values Calculated by Algorithms According to the Predicted Localizations

Variables	Origin	n	Mean	SD	*t*-value	*P*
PVC TZ score	RVOT	53	3.46	0.75	7.318	<.001*
	LVOT	63	2.44	0.74		
Sinus TZ score	RVOT	53	3.75	1.02	0.205	.838
	LVOT	63	3.71	1.02		
PVC QRS duration	RVOT	53	168.38	33.37	2.484	.014*
	LVOT	63	154.57	26.47		
PVC R wave duration in V1	RVOT	53	26.57	33.31	−0.412	.681
	LVOT	63	29.05	31.53		
PVC R wave duration in V2	RVOT	53	43.30	25.17	−1.726	.087
	LVOT	63	52.63	31.88		
PVC R wave deflection interval in V3	RVOT	53	48.09	20.69	−4.741	<.001*
	LVOT	63	65.76	19.39		
PVC R wave amplitude in V1	RVOT	53	0.11	0.15	−1.665	.099
	LVOT	63	0.18	0.25		
PVC S wave amplitude in V1	RVOT	53	1.41	0.61	5.248	<.001*
	LVOT	63	0.90	0.44		
PVC QRS amplitude in V1	RVOT	53	1.52	0.68	3.907	<.001*
	LVOT	63	1.08	0.55		
PVC R wave amplitude in V2	RVOT	53	0.28	0.27	−3.409	<.001*
	LVOT	63	0.53	0.47		
PVC S wave amplitude in V2	RVOT	53	1.92	0.70	6.409	<.001*
	LVOT	63	1.20	0.52		
PVC QRS amplitude in V2	RVOT	53	2.21	0.78	3.455	<.001*
	LVOT	63	1.73	0.70		
PVC R wave amplitude in V3	RVOT	53	0.67	0.35	−7.239	<.001*
	LVOT	63	1.39	0.65		
Sinus R wave amplitude in V2	RVOT	53	0.34	0.26	−0.285	.776
	LVOT	63	0.35	0.22		
PVC QRS amplitude in V2	RVOT	53	1.34	0.62	−0.687	.493
	LVOT	63	1.41	0.50		

Values are expressed as mean ± standard deviation (SD). Between-group comparisons were performed using independent *t*-test.
**P*-value <.05 was considered statistically significant.
LVOT, left ventricular outflow tract; PVC, premature ventricular complex; QRS, QRS complex duration; RVOT, right ventricular outflow tract; SD, standard deviation; TZ, transition zone.

Model validation showed that 84.4% of LVOT cases and 82.7% of RVOT cases were accurately classified, yielding a statistically significant distinction between groups ($P < .05$). The model achieved a sensitivity of 84.4%, specificity of 82.7%, PPV of 85.7%, and NPV of 81.1% (Table 8). Moreover, the Youden Index (0.66) exceeded that of the widely used V2S/V3R index. In the V3 transition subgroup, the model maintained a sensitivity of 92.1% and an NPV of 81.1%, with a Youden Index of 0.46—matching the V2S/V3R index and supporting the robustness of the model across challenging ECG patterns (Table 4).

Receiver-operating characteristic curve analyses were performed to evaluate and compare the classification performance of the 7 previously published algorithms and the newly developed supervised learning approach model. The new model demonstrated an AUC of 0.942 (Figure 4), significantly outperforming the AUCs of all individual algorithms in the overall population (Table 9). In the V3 transition subgroup, the model maintained a high discriminative ability with an AUC of 0.878 (Figure 5), again showing statistically superior

Table 4. Sensitivity, Specificity, Positive Predictive Value, and Negative Predictive Value Data of ECG Algorithms in All Patients and in V3 Transition Group

	All Patients				V3 Transition			
Algorithm	**Sensitivity 95% CI**	**Specificity 95% CI**	**PPV (%)**	**NPV (%)**	**Sensitivity 95% CI**	**Specificity 95% CI**	**PPV (%)**	**NPV (%)**
V2S/V3R index	69.8 (57.6-79.7)	94.3 (84.6-98.0)	93.6	72.4	71.1 (56.0-82.7)	75.3 (55.7-88.1)	82.2	62.1
TZ index	85.7 (75.0-92.3)	62.5 (49.0-74.3)	75.0	76.9	89.5 (76.7-95.9)	42.4 (25.5-61.0)	71.3	71.4
Combined TZ and V2S/V3R index	90.5 (80.8-95.6)	60.3 (46.9-72.3)	71.2	85.4	95.2 (84.2-98.8)	38.3 (22.2-57.4)	71.6	82.4
S and R wave difference in V1 and V2	53.9 (41.7-65.6)	92.4 (82.1-97.0)	89.4	62.8	45.1 (31.2-59.8)	88.2 (70.0-96.0)	85.3	50.2
R wave amplitude index in V1 combining with R wave deflection interval in V3	33.3 (22.9-45.6)	86.7 (75.0-93.4)	75.0	52.2	88.3 (74.9-95.0)	18.7 (8.4-36.0)	40.3	70.2
R wave duration index and R/S wave amplitude index	28.5 (18.8-40.6)	98.1 (90.0-99.7)	94.7	53.6	8.1 (3.0-20.1)	100.0 (85.1-100.0)	100.0	41.1
V2 transition ratio	69.8 (57.6-79.7)	64.1 (50.6-75.7)	69.8	64.2	68.0 (53.0-79.8)	67.3 (47.3-82.7)	76.5	57.1
New Algorithm	82.7 (71.6-90.1)	84.4 (72.4-91.8)	85.7	81.1	92.1 (80.1-97.1)	54.3 (36.6-71.0)	76.5	81.1

NPV, negative predictive value; PPV, positive predictive value; TZ, transition zone.

performance compared to the pre-existing algorithms (Table 10). These findings further support the robustness and generalizability of the proposed machine learning–based approach across both general and anatomically challenging subgroups.

DISCUSSION

In this study, the diagnostic performance of 7 previously published ECG-based algorithms were systematically compared with a newly developed supervised learning approach model using logistic regression. The new model integrated 4 significant predictors: PVC TZ score, PVC V2 R wave duration, PVC V3 R wave amplitude, and PVC V2 S wave amplitude.

Based on ROC curve analysis, the new algorithm achieved the highest discriminative ability with an AUC of 0.942 in the overall cohort and 0.878 in the V3 precordial transition subgroup. These values were significantly superior to all comparator algorithms ($P < .001$ for all), including the widely used V2S/V3R index (AUC = 0.103 and 0.158, respectively),

Table 5. Statistical Comparison of Ablation Region and Regions Predicted by ECG Localization Algorithms

		True RVOT		True LVOT			
Variables		**n**	**%**	**n**	**%**	**X^2**	***P***
TZ index	RVOT	17	32.1	1	1.6	18.15	<.001*
	LVOT	36	67.9	62	98.4		
R wave duration index and R/S wave amplitude index	RVOT	52	98.1	44	69.8	14.204	<.001*
	LVOT	1	1.9	19	30.2		
R wave amplitude index in V1 combining with R wave deflection interval in V3	RVOT	46	86.8	42	66.7	5.315	.016*
	LVOT	7	13.2	21	33.3		
V2 transition ratio	RVOT	34	64.2	19	30.2	12.069	<.001*
	LVOT	19	35.8	44	69.8		
V2S/V3R index	RVOT	50	94.3	19	30.2	46.575	<.001*
	LVOT	3	5.7	44	69.8		
Combined TZ and V2S/V3R index	RVOT	35	66.0	6	9.5	37.794	<.001*
	LVOT	18	34.0	57	90.5		
S and R wave difference in V1 and V2	RVOT	49	92.5	29	46.0	2.092	<.001*
	LVOT	4	7.5	34	54.0		

*$P < .05$ was considered statistically significant.
LVOT, left ventricular outflow tract; RVOT, right ventricular outflow tract; TZ, transition zone.

Table 6. Univariate Logistic Regression Analysis Results

		β	SE	Wald Statistics	P	OR
Step 1	PVC QRS duration	−0.011	0.014	0.579	.447	0.989
	PVC V1 R duration	−0.023	0.021	1.248	.264	0.977
	PVC V2 R duration	−0.078	0.027	8.394	.004	0.925
	PVC V3 R deflection interval	0.041	0.028	2.111	.146	1.042
	PVC V1 R amplitude	2.801	2.869	0.953	.329	16.458
	PVC V1 S amplitude	−0.823	0.739	1.241	.265	0.439
	PVC V2 R amplitude	1.244	2.623	0.225	.635	3.468
	PVC V2 S amplitude	−1.82	0.977	3.467	.063	0.162
	PVC V3 R amplitude	3.554	1.587	5.014	.025	34.944
	SINUS V2 R amplitude	−2.986	1.796	2.765	.096	0.05
	SINUS V2 QRS amplitude	0.413	1.022	0.163	.686	1.511
	PVC TZ score	−2.106	0.791	7.093	.008	0.122
	SINUS TZ score	−0.069	0.432	0.025	.873	0.933
	Still	10.264	3.782	7.365	.007	28695
Step 8	PVC V2 R duration	−0.06	0.018	10.99	.001*	0.942
	PVC V2 S amplitude	−1.958	0.665	8.673	.003*	0.141
	PVC V3 R amplitude	4.661	1.246	14.003	<.001*	105.73
	SINUS V2 R amplitude	−2.373	1.28	3.438	.064	0.093
	PVC TZ score	−2.036	0.74	7.57	.006*	0.131
	Still	8.436	2.918	8.36	.004*	4612

β, regression coefficient; OR, odds ratio; PVC, premature ventricular complex; SE, standard error; TZ, transition zone.
*$P < .05$ considered statistically significant.

the combined TZ and V2S/V3R index (AUC = 0.852 and 0.716), and the R wave–based indices by Okuyan[11] (AUC = 0.630 and 0.575). These results underscore the model's robustness across both general and anatomically challenging patient populations.

Collectively, these findings suggest that the integration of selected ECG features through a supervised learning model not only enhances classification accuracy across the full population but also sustains diagnostic performance in more nuanced ECG patterns such as precordial transition in V3. By contrast, rule-based algorithms, while useful, appear more limited in adaptability and may underperform when applied outside their original validation context.

Compared to traditional rule-based diagnostic methods, the supervised learning approach employed in this study offers several methodological and practical advantages.[11] By simultaneously evaluating and weighting multiple predictors based on statistical learning, this approach minimizes human bias in cutoff selection and improves the model's generalizability across varied populations. Logistic regression, a widely used supervised classifier, provides both predictive power and interpretability—2 qualities critical in clinical decision-making.[12] The model's consistent performance across the general cohort and the V3 precordial transition subgroup illustrates how data-driven approaches can enhance precision and reliability in electrophysiologic diagnostics. These findings are in line with previous reports demonstrating the superiority of supervised learning over conventional heuristics in clinical prediction tasks.

The supervised learning approach model's predictors were derived from PVC complexes, not sinus beats, proving ectopic ventricular activity alone can accurately differentiate between LVOT and RVOT origins. This emphasizes the importance of PVC-specific characteristics for data-driven localization tools. The model also does not rely on sinus rhythm–based precordial transition, which can be affected by cardiac rotation.[13] By focusing only on PVC features, the model is less impacted by anatomical variations and may be more reliable in diverse patient anatomies.

The present study reinforces the growing body of evidence suggesting that supervised learning approaches can outperform traditional rule-based algorithms in electrophysiological classification tasks. While rule-based models often rely on empirically determined cut-off values that may not generalize well across diverse patient cohorts, supervised models optimize parameter weighting based on statistical learning from labeled data.[14] This allows for improved adaptability to anatomical variability, particularly in anatomically ambiguous regions such as the aortomitral continuity.

An additional strength of the current model lies in its use of logistic regression, which provides not only robust predictive performance but also interpretability, an essential attribute in clinical decision-making. Unlike complex "black-box" models such as neural networks or ensemble classifiers, logistic regression enables clinicians to understand how each ECG variable contributes to the final classification.[15] This interpretability facilitates model acceptance among electrophysiologists and supports potential integration into clinical decision support systems.

The model's consistent performance across the general cohort and the V3 precordial transition subgroup illustrates how data-driven approaches can enhance precision and reliability in electrophysiologic diagnostics. A recent study by Zheng et al[15] proposed a machine learning-based method for localizing the origin of outflow tract PVCs using 12-lead ECG data. While both their study and ours share a common goal of improving diagnostic precision through machine

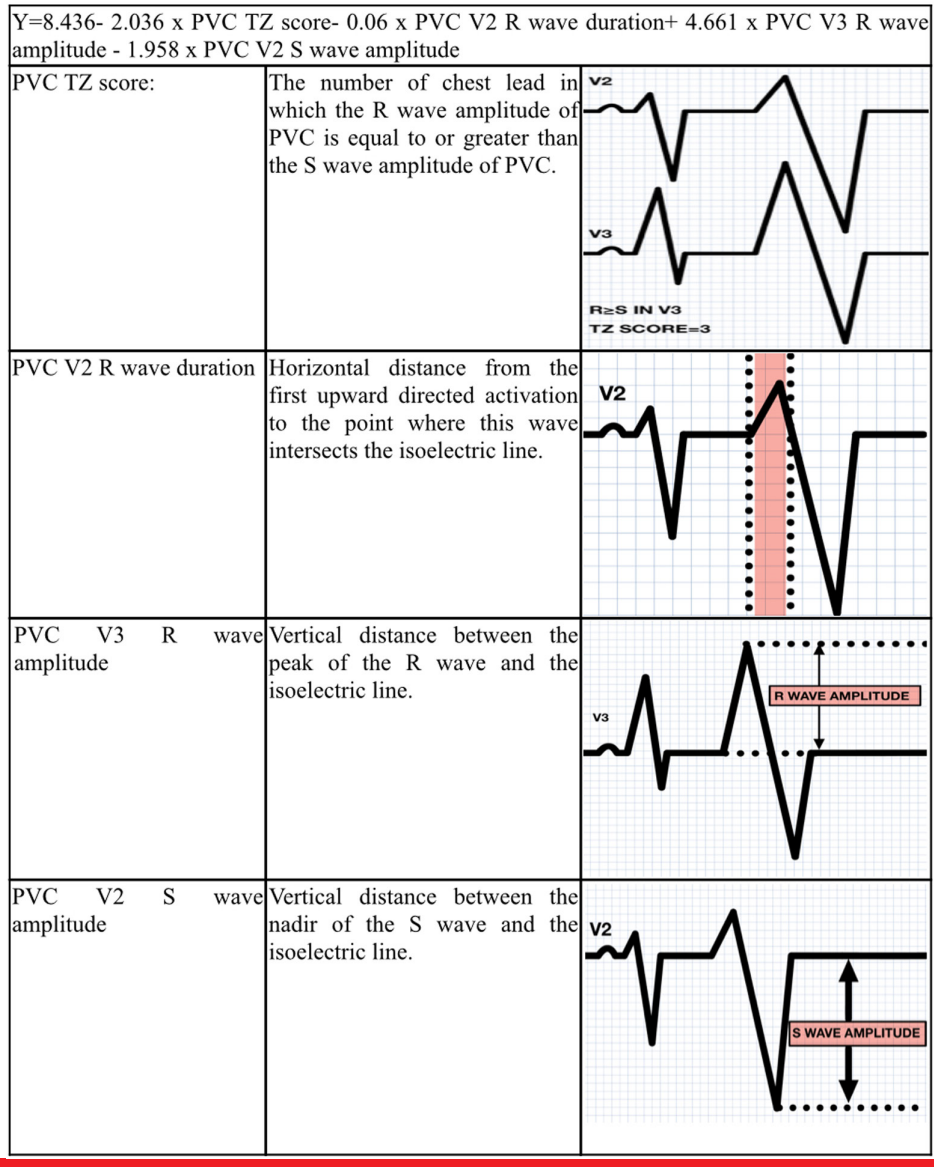

Figure 3. Electrocardiographic (ECG) measurements of new supervised learning approach model. Illustration of the 4 ECG parameters used in the model: premature ventricular complex (PVC) transition zone (TZ) score, PVC V2 R-wave duration, PVC V3 R-wave amplitude, and PVC V2 S-wave amplitude.

learning, key methodological differences exist. Zheng et al[15] employed an ensemble learning model based on XGBoost, a decision tree–based algorithm, incorporating more than 50 automatically extracted ECG features. In contrast, the approach utilized a supervised learning model constructed with a smaller number of clinically established features derived from 7 previously published ECG algorithms. In addition, the recent systematic review by Moreno-Sánchez et al[14]

Table 7. Average, Minimum and Maximum Values of "Y" in RVOT and LVOT Groups in the Newly Created Model Y = 8.436 − 2.036 × PVC TZ Score − 0.06 × PVC V2 R Wave Duration + 4.661 × PVC V3 R Wave Amplitude − 1.958 × PVC V2 S Wave Amplitude

	Average	Maximum	Minimum
RVOT	−2.25	0.49	−7.54
LVOT	4.64	13.35	0.53

LVOT, left ventricular outflow tract; RVOT, right ventricular outflow tract.

Table 8. Comparison of the New Machine Learning Algorithm with Ablation Sites

Predicted Origin (New Algorithm)†	True RVOT, n (%)	True LVOT, n (%)	χ^2	*P*
RVOT	43 (82.7)	10 (15.6)	49.338	<.001*
LVOT	9 (17.3)	54 (84.4)		

*$P < .05$ considered statistically significant.
LVOT, left ventricular outflow tract; RVOT, right ventricular outflow tract.
†The logistic regression formula was Y = 8.436 − 2.036 × PVC TZ score − 0.06 × PVC V2 R-wave duration + 4.661 × PVC V3 R-wave amplitude − 1.958 × PVC V2 S-wave amplitude. A threshold of Y > 0.5 was used to predict LVOT origin.

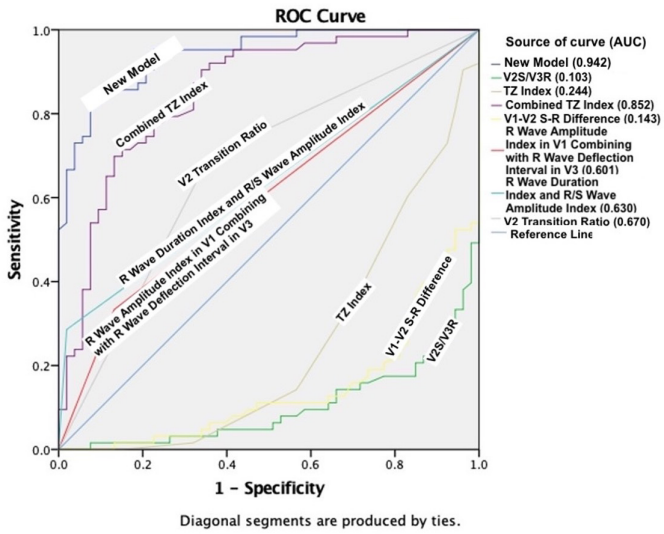

Figure 4. Receiver-operating characteristic (ROC) curve analysis of electrocardiographic (ECG) algorithms in all patients. Comparison of the diagnostic performance [area under the curve (AUC) values] of the newly developed supervised learning approach model with 7 established ECG algorithms.

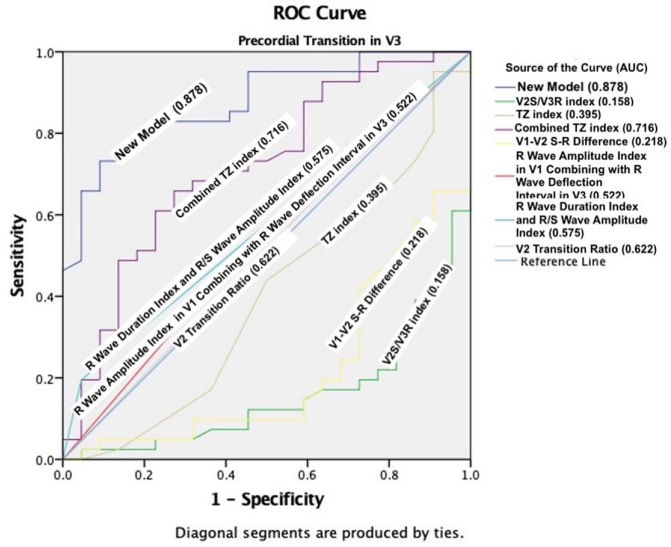

Figure 5. Receiver-operating characteristic (ROC) curve analysis in patients with precordial transition at lead V3. Subgroup analysis ROC curve analysis of algorithms in the V3 transition subgroup showing the discriminative ability of the new supervised learning approach model vs. existing electrocardigraphic algorithms in the diagnostically challenging V3 transition subgroup.

highlighted the rapid expansion of artificial intelligence (AI)-based ECG interpretation and emphasized the importance of interpretable, physiology-grounded models, further supporting the relevance of the feature-based supervised learning framework.

This distinction highlights a major strength of the method—clinical interpretability. Because each variable in the model corresponds to well-known diagnostic ECG criteria, the model's decision-making process can be better understood and trusted by clinicians. Moreover, unlike the Zheng et al[15] study, which did not assess model performance in clinically relevant subgroups, an additional analysis was conducted in patients with a transitional lead at V3, further demonstrating the robustness of the model across heterogeneous presentations. Lastly, the use of backward stepwise logistic regression based on the Wald statistic provided a statistically grounded feature selection process, resulting in a streamlined and explainable model architecture. In practical terms, the model can be applied by measuring 4 routinely available ECG parameters and entering them into the logistic regression formula to estimate LVOT probability. This could be easily implemented as a simple web-based calculator or integrated into ECG analysis or mapping systems for real-time use.

Recent advances in interpretable AI further underscore the transition from rule-based ECG criteria toward data-driven electrophysiologic analysis. For example, an ECG-only explainable deep-learning model developed by van de Leur et al[16] successfully predicted malignant ventricular arrhythmias in phospholamban cardiomyopathy, demonstrating how contemporary AI systems can extract prognostic and morphological signals beyond traditional ECG heuristics. Similarly, Bhatia et al[17] applied a convolutional deep-learning

Table 9. AUC Values of ECG Algorithms in all Patients

				Asymptotic 95% CI	
Test Result Variable(s)	**AUC**	**Standard Error**	***P***	**Lower Bound**	**Upper Bound**
New algorithm	0.942	0.020	<.001	0.903	0.980
V2S/V3R Index	0.103	0.029	<.001	0.046	0.159
TZ index	0.244	0.046	<.001	0.155	0.334
Combined TZ and V2S/V3R Index	0.852	0.036	<.001	0.781	0.923
S and R wave difference in V1 and V2	0.143	0.034	<.001	0.076	0.209
R wave amplitude index in V1 combining with R wave deflection interval in V3	0.601	0.052	.063	0.498	0.703
R wave duration index and R/S wave amplitude index	0.633	0.051	.014	0.533	0.734
V2 transition ratio	0.670	0.051	.002	0.570	0.770

AUC, area under the curve; TZ, transition zone.

Table 10. AUC Values of ECG Algorithms in V3 Transition

Test Result Variable(s)	AUC	Standard Error	*P*	Asymptotic 95% CI	
				Lower Bound	Upper Bound
New algorithm	0.878	0.042	<.001	.795	0.961
V2S/V3R index	0.156	0.049	<.001	0.060	0.253
TZ index	0.395	0.077	.171	0.245	0.545
Combined TZ and V2S/V3R index	0.716	0.069	.005	0.582	0.851
S and R wave difference in V1 and V2	0.218	0.060	<.001	0.099	0.336
R wave amplitude index in V1 combining with R wave deflection interval in V3	0.522	0.076	.773	0.372	0.672
R wave duration index and R/S wave amplitude index	0.575	0.073	.330	0.431	0.719
V2 transition ratio	0.511	0.077	.885	0.360	0.662

AUC, area under the curve; TZ, transition zone.

framework to intracardiac electrograms from subcutaneous Implantable Cardioverter Defibrillators (ICD) and showed that upstream intracardiac electrogram segments could predict ventricular arrhythmias with excellent performance, highlighting the potential of device-based signals for proactive, AI-driven arrhythmia prediction.[17] These advances highlight the growing movement toward explainable and physiology-driven AI in cardiac electrophysiology. The study aligns with—and contributes to—this shift by demonstrating that interpretable, feature-based models can outperform traditional rule-based algorithms while remaining fully transparent and clinically usable.

One major limitation of this study is its retrospective and single-center design, which may restrict the external generalizability of the findings. In addition, the sample size (n = 116) is modest for a supervised learning analysis and may increase the risk of overfitting. Because the primary objective was to derive a classification model rather than to perform full model validation, the entire dataset was used for model development without a separate training–testing split or cross-validation. Accordingly, all reported AUC values were derived from the same dataset. Thus, the present work should be regarded as a derivation study rather than a fully validated predictive model. Similar to previously published ECG algorithms, this study represents a derivation model developed on a single dataset without cross-validation or an independent validation cohort.[6] Consequently, the reported performance metrics should be interpreted with caution, and prospective validation in independent, multicenter cohorts is essential to assess the model's robustness across diverse anatomical and demographic profiles. Furthermore, only cases with successful ablation were included to ensure definitive localization of PVC origin based on electrophysiologic and ablation endpoints. While this design strengthens internal validity, it may introduce selection bias and limit generalizability to patients who are not candidates for ablation or in whom ablation is unsuccessful.

Another limitation is the absence of interobserver variability analysis, as all ECG measurements were performed by a single investigator. While this approach ensured internal consistency, it precludes the assessment of reproducibility and operator dependence, which are critical factors

Table 11. Comparison of AUCs in all Patients and V3 Transition Subgroup

Group	AUC of New Algorithm	Compared Algorithm	AUC of Compared Algorithm	*P*
All patients	0.942	V2S/V3R index	0.103	<.001
		TZ index	0.244	<.001
		Combined TZ and V2S/V3R index	0.852	<.05
		S and R wave difference in V1 and V2	0.143	<.001
		R wave amplitude index in V1 combining with R wave deflection interval in V3	0.601	<.001
		R wave duration index and R/S wave amplitude index	0.630	<.001
		V2 transition ratio	0.670	<.001
Precordial transition in V3	0.878	V2S/V3R index	0.158	<.001
		TZ index	0.395	<.001
		Combined TZ and V2S/V3R index	0.716	<.05
		S and R wave difference in V1 and V2	0.218	<.001
		R wave amplitude index in V1 combining with R wave deflection interval in V3	0.522	<.001
		R wave duration index and R/S wave amplitude index	0.575	<.001
		V2 transition ratio	0.622	<.001

AUC, area under the curve; TZ, transition zone

for real-world application. Future studies should incorporate blinded dual-reviewer measurements with inter-rater agreement metrics such as Cohen's kappa.

Although electroanatomical mapping and fluoroscopic guidance were employed to localize PVC origins during ablation, advanced imaging modalities such as intracardiac echocardiography (ICE) and cardiac magnetic resonance imaging (MRI) were not utilized. While ICE can enhance anatomical visualization and catheter-tissue contact in real time, particularly in complex ventricular anatomy, cardiac MRI may provide adjunctive information about myocardial fibrosis or intramural foci in selected patients. Although neither modality is routinely required for PVC ablation, their absence may have limited anatomical precision in certain challenging cases, such as those involving the LV summit or ambiguous epicardial sites.

It should also be noted that the diagnostic performance of previously published algorithms can vary significantly depending on the study population, operator experience, and methodological design. Therefore, even well-validated algorithms may perform differently across patient groups. Consistent with this, the findings of the study may not be directly generalizable to other populations without external validation.

Lastly, while the model developed in this study demonstrated superior diagnostic performance, it does not introduce entirely novel ECG parameters. Instead, it represents a re-analysis and re-integration of previously described ECG features using a supervised learning approach. This method allows for a more objective and data-driven synthesis of existing knowledge, enhancing diagnostic accuracy through statistical modeling rather than heuristic cutoff values.

CONCLUSION

The supervised learning approach model developed in this study—based on logistic regression—integrated 4 PVC-specific ECG features: TZ score, V2 R wave duration, V3 R wave amplitude, and V2 S wave amplitude. Compared to 7 previously established algorithms, the model demonstrated superior diagnostic accuracy, yielding the highest AUC in both the overall cohort and the diagnostically challenging V3 transition subgroup. Its data-driven framework, anchored in clinically interpretable variables, enables more precise and noninvasive localization of PVC origins, thereby enhancing the efficacy and targeting of catheter ablation procedures. Future work should focus on external validation across larger multicenter populations and the integration of this model into real-time clinical decision support systems.

Ethics Committee Approval: This study was approved by the Ethics Committee of Hacettepe University Faculty of Medicine on January 19, 2021 (Approval Number: GO 21/79, 2021/02-43).

Informed Consent: Informed consent was waived due to the retrospective design of the study.

Peer-review: Externally and internally peer-reviewed.

Author Contributions: Conception – A.S., C.Ç., A.K.; Design– A.S., C.Ç., A.K., U.C.; Supervision – H.Y., K.A., A.H.A.; Resources – H.Y., K.A.; Materials – N.O., A.K.; Data Collection and/or Processing– A.S., C.C., N.O.; Analysis and/or Interpretation – A.S., C.C., A.K., U.C.; Literature Review – A.S., C.Ç., N.O.; Writing – Original Draft: A.S., C.Ç., A.K.; Critical Review – All authors.

Acknowledgments: No generative artificial intelligence or AI-assisted technology was employed in the preparation, writing, or editing of this article. All content is the authors' original work.

Declaration of Interests: The authors have no conflicts of interest to declare. Dr. Necla Ozer is a member of the Editorial Board of this journal. She was not involved in the review or decision process of this manuscript.

Funding: The authors declare that this study received no financial support.

REFERENCES

1. Keleş N, Kahraman E, Parsova KE, Baştopçu M, Karataş M, Yelgeç NS. Does premature ventricular complex impair left ventricular diastolic functions? *Anatol J Cardiol*. 2023;27(4):217-222. [CrossRef]
2. Ito S, Tada H, Naito S, et al. Development and validation of an ECG algorithm for identifying the optimal ablation site for idiopathic ventricular outflow tract tachycardia. *J Cardiovasc Electrophysiol*. 2003;14(12):1280-1286. [CrossRef]
3. Betensky BP, Park RE, Marchlinski FE, et al. The V2 transition ratio: a new electrocardiographic criterion for distinguishing left from right ventricular outflow tract tachycardia origin. *J Am Coll Cardiol*. 2011;57(22):2255-2262. [CrossRef]
4. Yoshida N, Inden Y, Uchikawa T, et al. Novel transitional zone index allows more accurate differentiation between idiopathic right ventricular outflow tract and aortic sinus cusp ventricular arrhythmias. *Heart Rhythm*. 2011;8(3):349-356. [CrossRef]
5. Cheng Z, Cheng K, Deng H, et al. The R-wave deflection interval in lead V3 combining with R-wave amplitude index in lead V1: a new surface ECG algorithm for distinguishing left from right ventricular outflow tract tachycardia origin in patients with transitional lead at V3. *Int J Cardiol*. 2013;168(2):1342-1348. [CrossRef]
6. Yoshida N, Yamada T, McElderry HT, et al. A novel electrocardiographic criterion for differentiating a left from right ventricular outflow tract tachycardia origin: the V2S/V3R index. *J Cardiovasc Electrophysiol*. 2014;25(7):747-753. [CrossRef]
7. He Z, Liu M, Yu M, et al. An electrocardiographic diagnostic model for differentiating left from right ventricular outflow tract tachycardia origin. *J Cardiovasc Electrophysiol*. 2018;29(6):908-915. [CrossRef]
8. Kaypakli O, Koca H, Sahin DY, Karataş F, Ozbicer S, Koç M. S-R difference in V1-V2 is a novel criterion for differentiating the left from right ventricular outflow tract arrhythmias. *Ann Noninvasive Electrocardiol*. 2018;23(3):e12516. [CrossRef]
9. Bozyel S, Şimşek E, Koçyiğit Burunkaya D, et al. Artificial intelligence-based clinical decision support systems in cardiovascular diseases. *Anatol J Cardiol*. 2024;28(2):74-86. [CrossRef]
10. Hancock EW, Deal BJ, Mirvis DM, et al. American College of Cardiology Foundation; Heart Rhythm Society. AHA/ACCF/HRS recommendations for the standardization and interpretation of the electrocardiogram: part V. *J Am Coll Cardiol*. 2009;53(11):992-1002. [CrossRef]
11. Okuyan E. Big data in cardiology. *Anatol J Cardiol*. 2019;22(2):23-24. [CrossRef]

12. Patel S, Kwak L, Agarwal SK, et al. Counterclockwise and clockwise rotation of QRS transitional zone: prospective correlates of change and time-varying associations with cardiovascular outcomes. *J Am Heart Assoc*. 2017;6(11):e006281. [CrossRef]
13. Kırboğa KK, Küçüksille EU. Identifying cardiovascular disease risk factors in adults with explainable artificial intelligence. *Anatol J Cardiol*. 2023;27(11):657-663. [CrossRef]
14. Moreno-Sánchez PA, García-Isla G, Corino VDA, et al. ECG-based data-driven solutions for diagnosis and prognosis of cardiovascular diseases: a systematic review. *Comput Biol Med*. 2024;172:108235. [CrossRef]
15. Zheng J, Fu G, Abudayyeh I, et al. A high-precision machine learning algorithm to classify left and right outflow tract ventricular tachycardia. *Front Physiol*. 2021;12:641066. [CrossRef]
16. van de Leur RR, de Brouwer R, Bleijendaal H, et al. ECG-only explainable deep learning algorithm predicts the risk for malignant ventricular arrhythmia in phospholamban cardiomyopathy. *Heart Rhythm*. 2024;21(7):1102-1112. [CrossRef]
17. Bhatia NK, Koscova Z, Rogers AJ, et al. ID: 4120879 Deep learning approaches for prediction of ventricular arrhythmias using upstream electrograms from intracardiac devices. *Heart Rhythm*. 2024;21(9):S774. [CrossRef]